20th Annual Conference of the Canadian Nuclear Society
Montreal, Quebec, Canada / May 30 - June 2, 1999

DYNAMIC RESPONSE OF THE SDS FLOW-MEASUREMENT SYSTEM IN CANDU

by
V.T. Koslowsky, H.W. Hinds, P.D. Tonner and O. Glöckler (Ontario Power Generation)
Atomic Energy of Canada Ltd., Chalk River, Ontario K0J 1J0
1999 April

1. BACKGROUND

Safety analyses of design basis accidents place upper limits on the dynamic response of safety-related flow-measurement equipment in CANDU. This study was initiated by the Loss-Of-Flow (LOF) trip-coverage improvement project at Darlington Nuclear Generating Division (DNGD), Ontario Hydro, where, in the fall of 1997 a program was instituted to measure, readjust and validate the response time of the primary heat transport (PHT) safety system flow transmitters across all 4 units with non-intrusive, *in-situ,* flow-noise measurements. This report summarizes the methods developed for flow-noise analysis and describes results of tests to ensure the validity of underlying assumptions in this type of analysis.

At each Darlington nuclear generating unit, two safety shutdown systems (SDS1 and SDS2) monitor PHT coolant flow in 24 of the 480 inlet feeders. In these feeders, the flow is determined from the pressure drop across an orifice that obstructs 36% of the pipe cross-sectional area. The pressure drop is measured with a differential-pressure (DP) cell, which for serviceability is located outside the reactor vault, 35 to 45 m away from the high-radiation fields at the orifice. The pressure upstream and downstream of the orifice plate is transferred to the DP cell by a pair of steel instrument tubes, often called impulse lines. In effect, a flow-measurement system comprises the orifice plate, the pair of impulse lines from the high and low pressure sides of the orifice, and the DP cell with its 4-to-20 mA current transmitter. Careful analysis of *in-situ* flow-signal fluctuations, commonly called flow noise, gathered from the transmitter through a high-fidelity data-acquisition system, such as those constructed by AECL, can reveal attributes of the entire flow-measurement system.

Figure 1 shows the DP signals typical of SDS1 and SDS2 in the two left panels. The spectral content of these signals is shown, on the right of this figure, as a power spectral density (PSD). The oscillations clearly evident in the time-domain manifest themselves as peaks in the PSD. For example, the Rosemount (SDS1) transmitter signal exhibits an 8 Hz oscillation while the Gould (SDS2) exhibits a 4 Hz oscillation. Both oscillations are seen as the fundamental resonances in their respective PSDs. The SDS2 signals are also noisier than the SDS1 signals. The spectral content of the SDS2 signal, above 1 Hz, is two to three decades larger in power than that of the SDS1 signal. The frequency content above 1 Hz is responsible for the noisy SDS2 behaviour. The solid line underlying each PSD in Figure 1, shifted down for clarity, represents a parameterized model of the transmitter PSD. The response time of the transmitter can be deduced from the model parameters that provide the best fit to the data.

The accuracy of determining transmitter response times with this technique depends on the suitability of the model; the ability to deconvolve the interfering effects of impulse-line resonances; and the validity of an underlying assumption that the acoustic noise entering the measurement system be "white", i.e. have a uniform, broad-band spectral content.

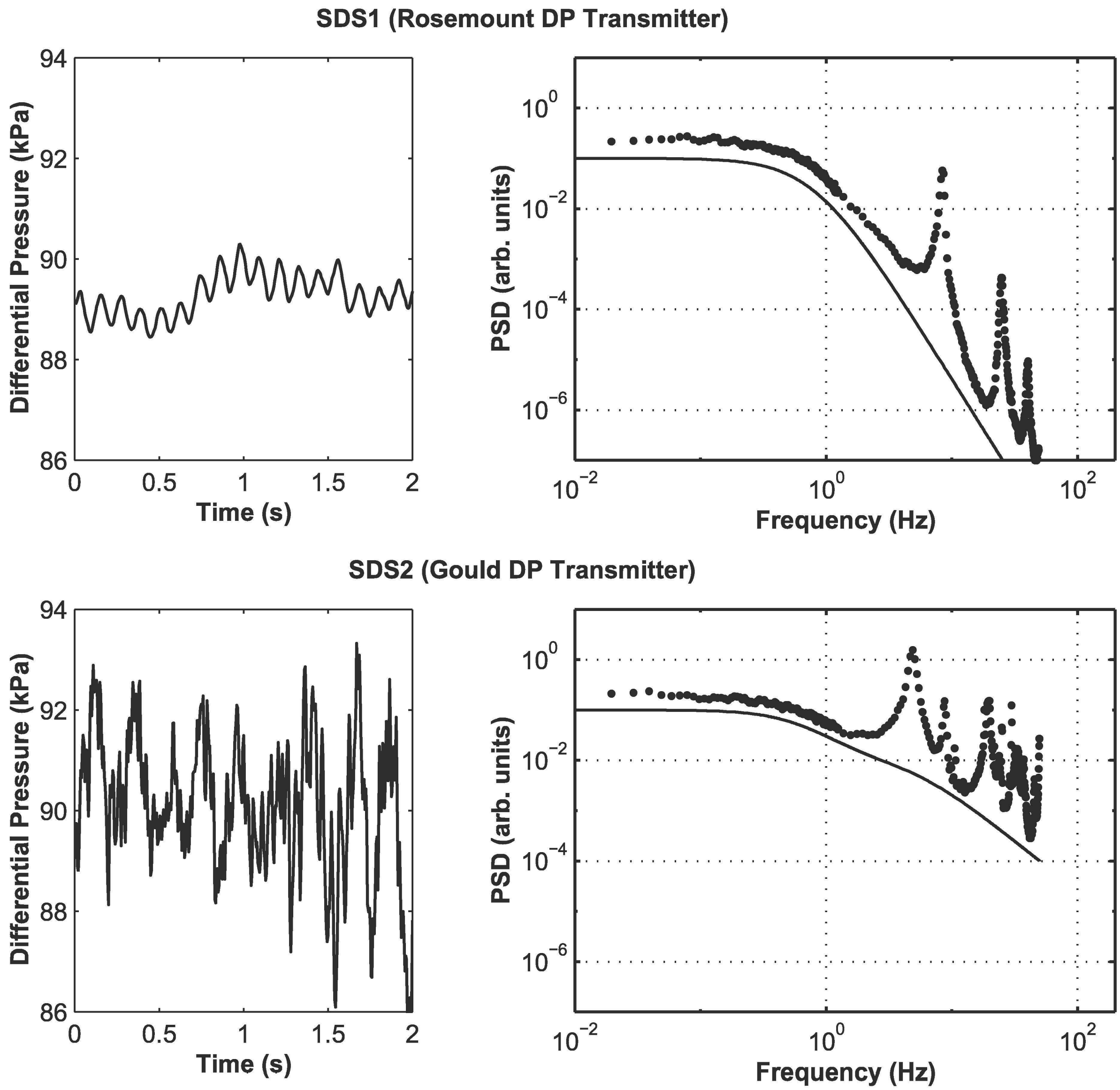

Figure 1: Samples of SDS1 (Rosemount) and SDS2 (Gould) DP-transmitter signals are shown in the left panels. The spectral content of these signals are shown on the right.

2. MODEL VALIDATION

If the transmitter response is linear, then the response time of a transmitter is linearly related to its transfer function time constants (see Table 1), provided a realistic model or parameterization of the transmitter is chosen. The models of the dynamic response of Rosemount, Gould and Bailey DP transmitters, the first two of which are commonly used in CANDU stations, have been determined through a set of special, *in-situ*, signal measurements by simultaneously recording the hydraulic signals entering the DP cell with a pair of temporarily installed high-frequency pressure transducers (Piezotronics model ICP 101A06) and the outgoing DP-transmitter signal. The signals were sampled with the AECL-built noise-analysis system (NAS), which features electrical isolation through the use of optically-coupled amplifiers, dc-offset adjustments, individual-channel adjustable gains, anti-aliasing low-pass filters, 16-bit analog-to-digital conversion and selectable sampling frequency from 1 to 2400 Hz. During the DNGD tests, sampling frequencies of 10, 25, 200 and 2400 Hz were used. The transmitter response function is calculated as the ratio of the Fourier components of the incoming signal, derived from the difference in ICP signals, and the Fourier components of the DP signal. These response functions are shown in Figure 2. Transfer functions of the Rosemount, Gould and Bailey DP transmitters were determined [1] by parameterizing the measured response functions, as a ratio of polynomials in *s*, the Laplace variable.

Table 1: Transfer Functions for Rosemount, Gould and Bailey DP Transmitters

Transmitter	Transfer function	Response Time (ms)	Typical values
Rosemount	$\frac{1}{(1+s\tau_a)}\cdot\frac{1}{(1+s\tau_b)}\cdot\frac{1}{(1+s\tau_c)}$	$\tau_a+\tau_b+\tau_c$	$\tau_a = 85.6$ ms $\tau_b = 30.8$ ms $\tau_c = 3.9$ ms
Gould	$\frac{(1+s\tau_d)}{(1+s\tau_a)(1+2\varsigma s\tau_c+s^2\tau_c^2)}$	$\tau_a-\tau_d+2\cdot\varsigma\cdot\tau_c$	$\tau_a = 351.2$ ms $\tau_c = 1.252$ ms $\tau_d = 94.78$ ms $\zeta = 0.5995$ prompt fraction $= \tau_d/\tau_a$
Bailey	$\frac{1}{(1+s\tau_a)\cdot(1+s\tau_b)\cdot(1+2\varsigma s\tau_c+s^2\tau_c^2)}$	$\tau_a+\tau_b+2\cdot\varsigma\cdot\tau_c$	$\tau_a = 59.2$ ms $\tau_b = 12.3$ ms $\tau_c = 131.3$ ms $\zeta = 0.617$

The transfer functions that best describe the measured response functions are listed in Table 1 [1] and shown in Figure 2 as solid lines. The excellent fit of the models to the data suggests that the response time of the transmitters can be reliably inferred from these parameterizations of the response function. The identical parameterization, squared, underlies the measured PSD. However, it can only be obtained after reliably deconvolving the impulse-line resonances. In addition, the incoming hydraulic noise cannot normally be measured. Consequently, when analyzing PSDs, there is an inherent assumption that the spectral content of the incoming pressure noise is constant and broad-band.

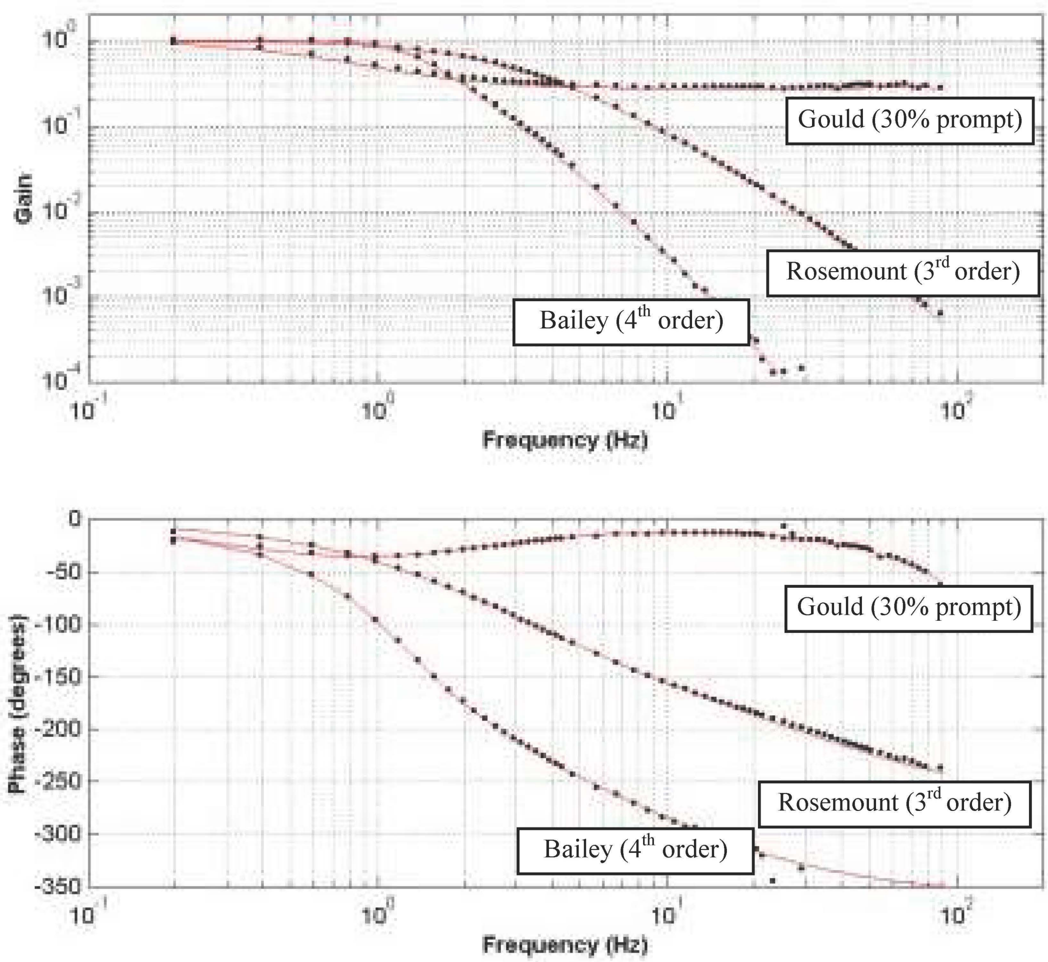

Figure 2: The measured response-function gain and phase for three types of DP transmitters are shown as points. The lines represent a fit of the models, listed in Table 1, to the data.

3. IMPULSE-LINE MODELLING

Impulse-line dynamics can be mathematically modelled [2] as hydraulic transmission lines analogous to that found in electrical transmission theory except that the impedance and propagation terms are viscosity dependent. The general solution has the form:

$$P(x,s) = A(s)\cdot e^{-\Gamma(s)\cdot x} + B(s)\cdot e^{\Gamma(s)\cdot x} \tag{1}$$

$$Q(x,s) = \frac{A(s)\cdot e^{-\Gamma(s)\cdot x} - B(s)\cdot e^{\Gamma(s)\cdot x}}{Z(s)} \tag{2}$$

where

P(x, s) describes the pressure at a position, *x*, along the transmission line (Pa) ;
Q(x, s) describes the flow rate at a position, *x*, along the transmission line ($m^3 \cdot s^{-1}$) ;
Z(s) is the characteristic impedance of the transmission line ($Pa \cdot s \cdot m^{-3}$) ;
Γ(s) is the propagation factor (m^{-1}) ;
s is the complex frequency $j \cdot 2\pi f$;
f is the frequency (Hz);
j is the square root of –1; and
x is the position along the transmission line (m).

Expressions for *Z(s)* and *Γ(s)* are listed in Table 2 and the parameter values required for their evaluation are listed in Table 3 for Darlington impulse-line conditions. The impedance, *Z(s)*, and propagation factor, *Γ(s)*, used in this work were obtained from Rzentkowski *et al.* [3], and represent a thin-walled elastic conduit that is filled with a viscous fluid and anchored against movement along its length. Boundary conditions, such as the flow at the end of the transmission line or the initial pressure at the entrance to the transmission line, permit the amplitudes, *A(s)* and *B(s)*, to be calculated.

The model of the Darlington flow-measurement system consists of a pair of hydraulic transmission lines, approximately 45 m long, mismatched in length by about 0.75 m, terminating in either a Rosemount (SDS1), Gould (SDS2) or Bailey (SDS2 replacement candidate) DP cell. The pressures at the ends of the impulse lines differ by the DP-cell pressure. The relationship between the integrated flow into the DP cell and the differential-pressure across the cell is:

$$\frac{Q}{s} = DP(s) \cdot C \tag{3}$$

where

$\frac{Q}{s}$ is the integrated flow (in Laplace space) through the DP cell;
DP(s) is the differential pressure signal across the cell; and
C is the compliance of the DP cell.

The compliance represents the displaced volume of the DP cell, normalized to the imposed differential pressure. Evidence from measurements at Darlington [4] indicate that the compliance for the Gould and Bailey DP cells is of order 10^{-12} m^3 / Pa, in agreement with the technical specifications provided by the manufacturers. The Rosemount is best represented by a compliance of order 10^{-13} m^3 / Pa, an order of magnitude smaller than the Gould or Bailey DP cells.

Solution of the transmission equations can be formulated to provide a relationship between the differential pressure at the DP cell and the pressure and differential pressure at the orifice, $P_{orifice}$ and $DP_{orifice}$, respectively, viz.

$$DP(s) = P_{orifice}(s) \cdot T_P(s) + \Delta P_{orifice}(s) \cdot T_{\Delta P}(s) \tag{4}$$

where

T_P represents a complex transfer function between the high pressure at the orifice and differential pressure at the DP cell; and

$T_{\Delta P}$ represents a complex transfer function between the differential pressure at the orifice and differential pressure at the DP-cell inlet.

As an example, the predicted transfer function, T_P, and its measured response from tests performed on a water loop at Chalk River are shown in Figure 3 for the Rosemount transmitter. The agreement between measurement and model is quite good for the Rosemount DP cell. However, this is not the case for the Gould and Bailey DP cells (not shown). This disagreement is thought to be due to their larger compliance or the unsuitabilty of equation 3 in mathematically expressing the effect of the DP cell on the impulse line hydrodynamics.

4. FITTING IMPULSE-LINE AND TRANSFER FUNCTION MODELS TO MEASURED DARLINGTON POWER-SPECTRAL DENSITIES

Sections 2 and 3, above, have illustrated that reliable models of transfer functions and impulse lines exist for the Rosemount DP transmitter. These models can now be applied to PSDs of measured Rosemount-transmitter signals to determine their response times. However, first efforts to model the resonances from a Darlington DP transmitter failed to predict the higher-order impulse-line resonance frequencies properly. The model predicted the exact odd harmonic ratios, as expected from the physics of an open/closed resonating tube, but this was not observed on the DNGD impulse lines. This shortcoming was identified to be due to the lack of a large temperature gradient in the impulse-line model. Acoustic velocities and water viscosity in the impulse lines differ dramatically from the transmitter room, at 20°C, and the inlet to the impulse line, at 270°C, as shown in Table 3. When a slightly more sophisticated model of the impulse lines is used, consisting of one cold and one hot section, the results shown in Figure 4 are achieved. Many of the model parameters, listed to the right of the graph, are fixed material properties of water or steel. The parameters adjusted to achieve a reasonable fit are the transmitter time constants, τ_1, τ_2 and τ_3, the lengths of the hot and cold sections of impulse lines, the mismatch in impulse-line lengths, δL, and the pressure and differential-pressure noise, P and δP, respectively at the orifice plate.

5. RESPONSE-TIME ACCURACY FROM CURVE-FITS OF PSDS

An indication of the expected accuracy of the bi-temperature transmission-line model and curve-fit algorithm can be determined by comparing, for the same transmitter, the PSD curve-fit analysis and analyses of reference measurements. These were performed with either bench step-tests or *in-situ* noise measurements using the high-frequency-response, ICP transducers described in Section 2. The results of this intercomparison are displayed in Figure 5. The uncertainty in the reference response times was assumed to be ±10%. The uncertainties associated with the curve fits represent the scatter in the results when the parameters of the fit were altered by plausible estimates of the parameter uncertainties. Although this assessment must be more thoroughly conducted, the excellent agreement between analysis methods certainly warrants further validation efforts. The good agreement also suggests that the underlying assumption regarding the constant, broad-band hydraulic noise is valid for the flow channels utilized in this study.

Table 2: Model Conditions and Expressions for Darlington Impulse Lines

Symbol	Description	Expression
c_0	speed of sound in bulk water	$c_0 = \left(\frac{K}{\rho}\right)^{0.5}$
c	speed of sound in impulse line	$c = c_0\left(1+\psi\cdot\frac{K}{E}\right)^{-0.5}$
Ψ	parameter used in evaluating speed of sound, c	$\psi = 2(1+\mu)\frac{R^2 + r^2 - 2\cdot\mu\cdot r^2}{R^2 - r^2}$
Z	complex impedance of hydraulic transmission line	$Z(s) = \frac{\rho\cdot c}{\pi\cdot r^2}\left(1 - \frac{2\cdot J_1(j\cdot z(s))}{j\cdot z(s)\cdot J_0(j\cdot z(s))}\right)^{-0.5}$
s	Laplace variable equal to complex frequency	$s = j\cdot 2\pi\cdot f$
f	frequency	
q	viscosity-dependent term	$z(s) = r\left(\frac{s}{\nu}\right)^{0.5}$
j	square root of -1	$j = \sqrt{-1}$
Γ	complex propagation factor	$\Gamma(s) = \frac{s}{c}\left(1 - \frac{2\cdot J_1(j\cdot z(s))}{j\cdot z(s)\cdot J_0(j\cdot z(s))}\right)^{-0.5}$
J_0 and J_1	zero and first-order Bessel functions	

6. EFFECT OF FLOW-DIP SIGNALS: VIOLATION OF THE WHITE-NOISE ASSUMPTION

A small number of the SDS flow channels, across all four Darlington units, show large-negative, aperiodic flow-signal transients called "flow-dips". The Fourier amplitudes of these transients are not broad-band but attenuate quickly above 10 Hz. This can be established by Fourier analyzing only relatively quiet intervals of these DP signals and comparing the Fourier amplitudes with those obtained from the complete dataset.

Table 3: Properties of Darlington Impulse Lines

Property	Darlington N.G.S.
Length of Impulse Lines	~ 45 m
Length Mismatch	≤ 1 m
Operating Temperature	20°C at DP cell to 270°C at orifice plate
Operating Pressure	~10 MPa
Water Type	heavy
Density of water (ρ)	1110 kg/m^3 at 20°C 854 kg/m^3 at 270°C
Viscosity of Water (ν)	$1.21\cdot10^{-6}$ m^2/s at 20°C $1.29\cdot10^{-7}$ m^2/s at 270°C
Bulk modulus of water (K)	$2.1\cdot10^{9}$ Pa at 20°C $5.4\cdot10^{8}$ Pa at 270°C
Tubing Material	Steel
Young's modulus of Tubing (E)	$1.8\cdot10^{11}$ Pa at 20°C $1.9\cdot10^{11}$ Pa at 270°C
Poisson's Ratio of Tubing (μ)	0.29
Inner Diameter of Tubing (r)	7 mm
Outer Diameter of Tubing (R)	9.5 mm
Speed of Sound in Tubing (c)	1323 m/s at 20°C 787 m/s at 270°C

The effect of the flow-dip signals is, therefore, to raise the power of the PSD at low frequencies while leaving the high-frequency Fourier amplitudes unaltered, as illustrated in Figure 6. A second effect is to distort the shape of the knee of the PSD since the roll-off deviates significantly, on the log-log plot, from the expected straight line. Both of these effects introduce a large uncertainty in the deduced corner frequency or transmitter response time. Fortunately, the presence of flow-dip signals is easily identified by the onset of any skewness in the signal amplitude distribution, so precautionary measures, such as Fourier analysis of only quiet intervals of data, can be taken.

7. SUMMARY

This work illustrates that noise analysis can be a quantitative and non-intrusive surveillance technique for determining DP-transmitter response times from PSDs. When a sound understanding of the underlying principles of flow-noise generation are also applied, noise analysis can be extended to determine physical characteristics of the entire measurement system, for example, impulse-line temperature gradients.

8. REFERENCES

[1] H.W. Hinds, "Validation of the Auto-Power-Spectral-Density Method of Determining The Response Time of Rosemount, Gould And Bailey Flow Transmitters", COG-98-323-R0, 1998 December.

[2] R.E. Goodson and R.G. Leonard, "A Survey of Modeling Techniques For Fluid Lines Transients", J. of Basic Engineering, Trans. ASME, Vol. 94, No.2, p. 474-482, 1972 June.

[3] G. Rzentkowski, J.W. Forest and J.H. Russell, "Estimation of Pump-Generated Pressure Pulsations From Instrument Line Measurements", Ontario Hydro Research Division, Toronto, Canada.

[4] V.T. Koslowsky, H.W. Hinds and O. Glockler, "Effects of Instrument-Line Lengths on Differential Pressure Measurements", CS-NAH-TN-33, Rev. 0, 1998 November.

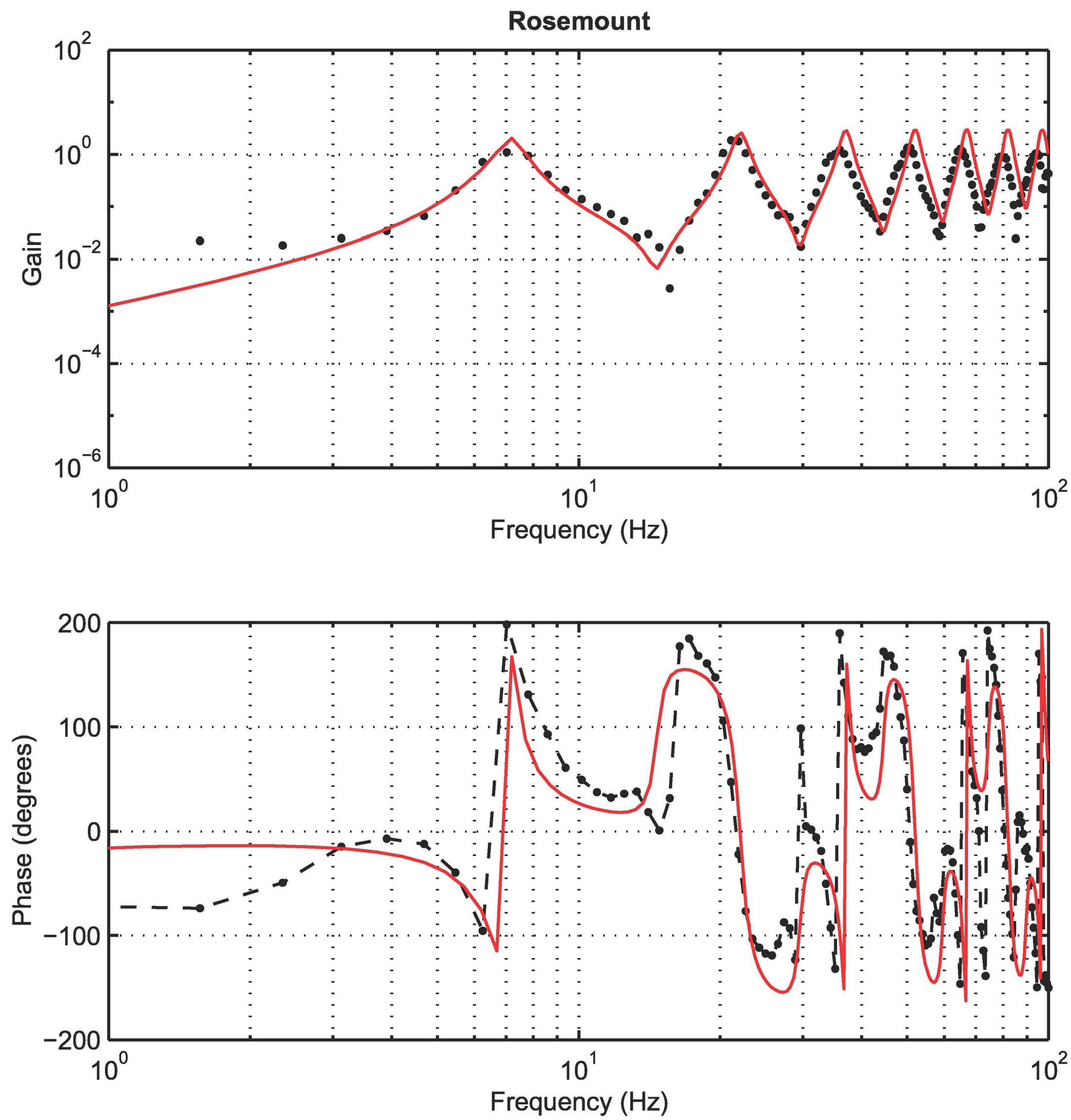

Figure 3: The measured response function and predicted pressure-dependent component of the transfer function, T_P, is shown for a differential-pair of impulse lines when a 1 m-long mismatch in 46 m of tubing exists. A Rosemount DP cell is attached to the end of the impulse lines in this measurement. Filled circles represent the results of measurements on the CRL test water loop while the line is a prediction using the model described in Section 3.

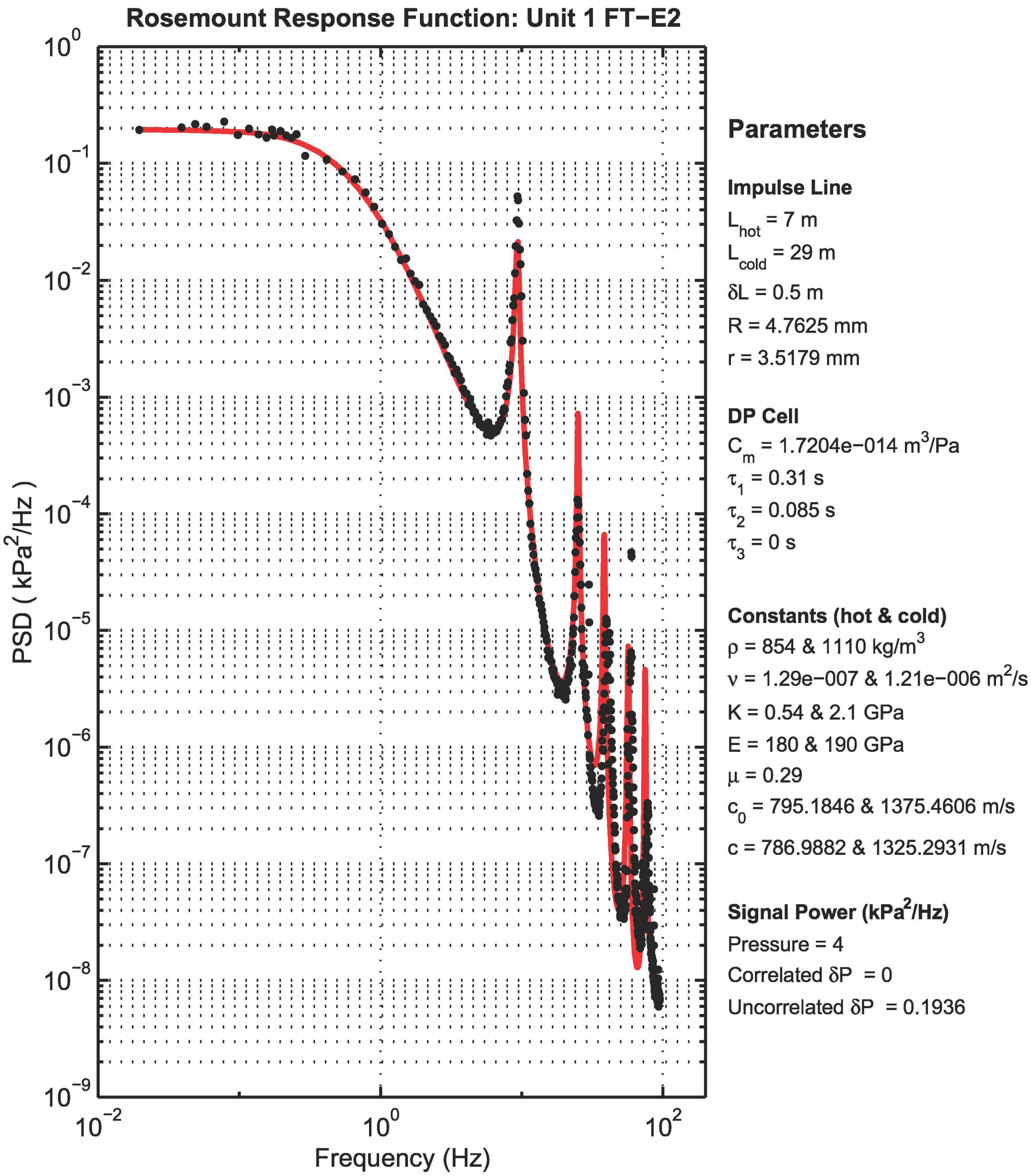

Figure 4: Prediction of the bi-temperature, transmission-line-model (solid line) is compared with the measured PSD of flow transmitter E2 at Darlington Unit 1(filled circles). The length of the hot portion of the impulse lines is comparable to the size of the feeder cabinet in which they are partially contained. The parameters, listed to the right of the graph were used to model the data.

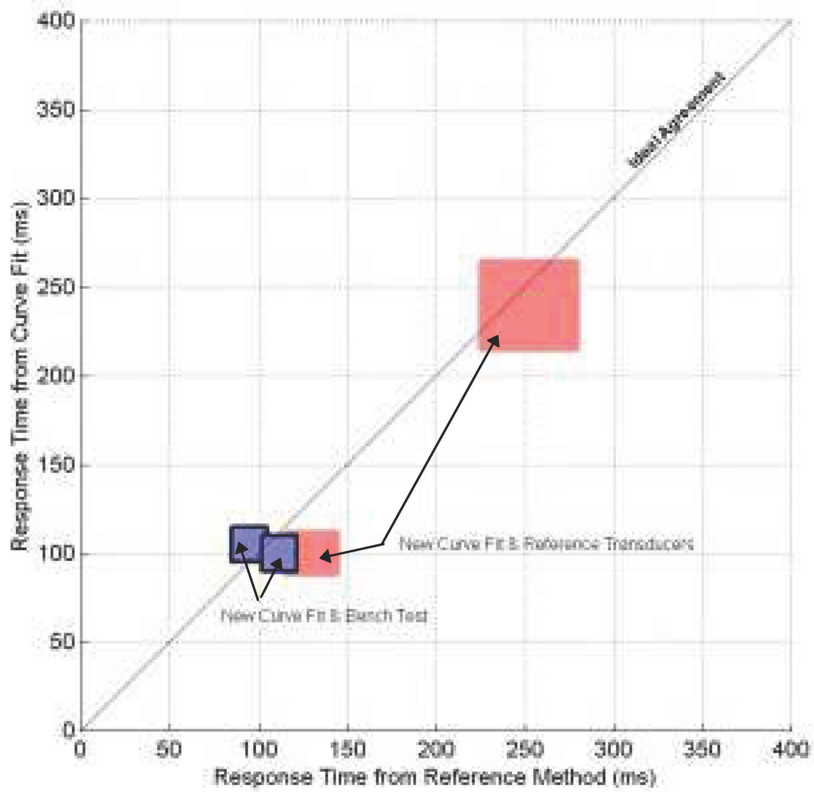

Figure 5: Three analysis techniques: a curve fit of the PSD calculated from *in-situ* flow-noise; pressure-step bench tests of a DP transmitter; and transfer function analyses with reference-transducer signals (as described in Section 2) are compared above for a Rosemount DP transmitter. The breadth of the shaded areas, in each dimension, is intended to reflect the uncertainties associated with the response-time determination. The agreement between reference methods and the curve fit of the PSD is excellent.

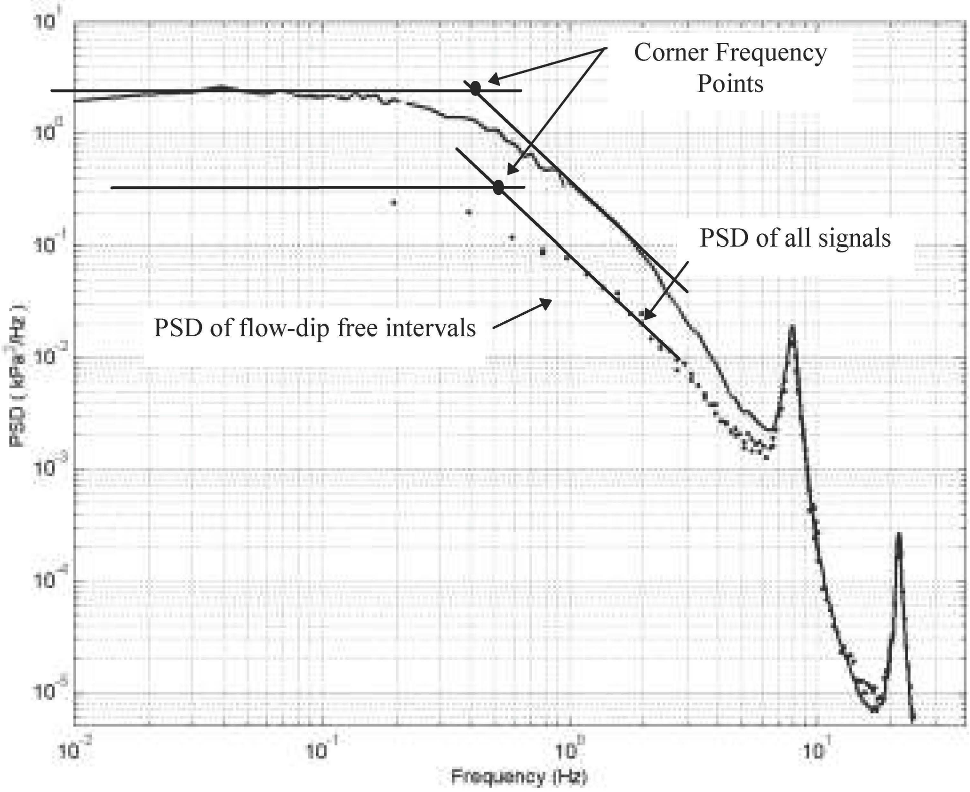

Figure 6: The distorting effect of flow-dip signals on the PSD is shown above. The PSD of a flow transmitter that is plagued with large-negative, aperiodic signal transients, known as flow-dip signals, is shown as a solid line. The PSD computed from flow-dip free intervals of the same data set is shown as points. Note that the high-frequency components of the two PSDs are similar, but that the plateau, in particular, has risen in the case of the solid line. The plateau of the lower PSD is similar to that found on normal flow channels. One effect of flow-dip signals, therefore, is to raise the low-frequency components of the PSD. A second effect is to distort the shape of the knee of the PSD, as seen above, since the roll-off deviates significantly from the expected straight line on the log-log plot. While the flow-dip free PSD has an easily defined corner-frequency, the PSD of the entire dataset does not. Consequently the response time of the transmitter that is deduced from the higher PSD is biased, either up or down depending on the subjectivity of the analyst.